DRUG FORMULATIONS AND CLINICAL METHODS

# Fractional Wavelet Analysis for the Simultaneous Quantitative Analysis of Lacidipine and Its Photodegradation Product by Continuous Wavelet Transform and Multilinear Regression Calibration

**ERDAL DINÇ**
Ankara University, Faculty of Pharmacy, Department of Analytical Chemistry, 06100, Tandoğan, Ankara, Turkey
**GAETANO RAGNO and GIUSEPPINA IOELE**
University of Calabria, Department of Pharmaceutical Sciences, 87036 Arcavacata di Rende, Cosenza, Italy
**DUMITRU BALEANU**
Çankaya University, Faculty of Arts and Sciences, Department of Mathematics and Computer Sciences, 06530, Ankara, Turkey and National Institute for Laser, Plasma and Radiation Physics, Institute of Space Sciences, Magurele-Bucharest, PO Box MG-23, R 76911, Romania

**Fractional wavelet transform (FWT) was applied to the original absorption spectra of lacidipine (LAC) and its photodegradation product (LACD), and the resulting FWT spectra were processed by continuous wavelet transform (CWT) and multilinear regression calibration (MLRC) for the simultaneous quantitative analysis of both products in their binary mixtures. These methods do not require any chemical separation step and chemical complex reaction to obtain a detectable signal for the degradation product. By using the Mexican hat function, 2 calibration functions for LAC and LACD were obtained by measuring the CWT transformed signals at 416.1 nm for LAC and 414.6 nm for LACD, after FWT processing of the original absorption spectra. The calibration graphs were linear in the concentration range of 5.08–40.64 μg/mL for LAC and 0.51–8.16 μg/mL for LACD. The limit of detection and the limit of quantitation were found to be 0.289 and 0.956 μg/mL for LAC and 0.036 and 0.118 μg/mL for LACD, respectively. For comparison, the MLRC algorithm was applied to the linear regression functions for the individual drug and its photoproduct. In this approach, a set of linear regression functions was obtained from the relationship between concentrations and FWT signals in the wavelength range 411.0–412.4 nm. Both methods were applied to the quantitative evaluation of LAC and LACD in laboratory and pharmaceutical samples, and produced very satisfactory results.**

Received December 11, 2005. Accepted by JM April 3, 2006.
Corresponding author's e-mail: dinc@pharmacy.ankara.edu.tr

Identification of impurities and degradation products during the pharmaceutical development process and after market is of interest because of science and business interests and also because of regulatory requirements. The drug and its degradation profiles give us a good understanding of the process or product.

The simultaneous determination of the components in pharmaceutical formulations having a low content of degradation products is one of the main challenges of analytical chemistry. For this reason, many analytical methods have been proposed for the chemical analysis of drugs, degradation products, and impurities. Most of these analytical methods may not produce good results in some cases, or the methods have expensive and difficult applications for solving the mentioned analytical problems. Finding new approaches for solving the above-mentioned drawbacks is a constant preoccupation of analytical chemistry and its related branches.

In our study, a binary composition consisting of lacidipine (LAC) and its photodegradation product (LACD) was investigated. LAC, having a dihydropyridine structure, is an antihypertensive drug that acts by blocking L-type calcium channels. The drug is extremely sensitive to light, as well as all other drugs belonging to the same chemical class (1–5). Recently, the detailed photochemical degradation process of the drug has been investigated (6). The drug is converted into its *cis* isomer, which in turn undergoes cyclization to give LACD. Analytical methods for the determination of LAC in pharmaceutical dosage forms, as well as in biological fluids, have been reported in literature (7–9). Drug stability tests were carried out by following the International Conference on Harmonization (ICH) recommendations for the photodegradation products (10).

Recently, the fractional wavelet approach was developed for solving various problems in several areas of science and engineering (11–15). The wavelet transform methods and their applications in analytical chemistry have significantly

Downloaded from https://academic.oup.com/jaoac/article/89/6/1538/5657781 by ANKARA UNIVERSITESI user on 11 December 2021

increased the potential power of various spectral techniques (16–17). The continuous wavelet transform (CWT) approach is a powerful signal-processing tool for data reduction, denoising, baseline correction, and resolution of multicomponent overlapping spectra. The CWT approach is very useful for the simultaneous quantitative analysis of multicomponent mixtures of drugs. The CWT method, in combination with different multivariate calibrations, has been used for analyzing complex mixtures (18–25). Multivariate calibration analysis (26–30) is a new and promising approach for quantitative analysis without using any graphical procedure.

The aim of this study is to develop analytical methods for the simultaneous quantitative analysis of LAC and LACD in their mixtures without using procedures such as separation, extraction, and complex reactions. In this analysis, the main problem was the low content of LACD. A partial least-squares (PLS) calibration was first applied to the original absorption spectra of LAC and LACD mixtures, but the results obtained showed particularly high errors for LACD assay. For these reasons, the fractional wavelet transform (FWT) approach was applied to the original absorption spectra to provide more highly detectable absorption signals and data reduction. Coefficients obtained by FWT were processed by the Mexican hat function, and the methods were validated. By using FWT spectra, the results obtained from the Mexican hat function and a multilinear regression calibration (MLRC) method were compared, and a very good agreement between data was observed.

## Theory

### *FWT Method*

A new wavelet transform based on the fractional B-splines was described (1–3). The splines played an important role in the early development of the theory of the wavelet transform. The generalization of the spline constructions was proposed (3), and new wavelet bases with a continuous order parameter were obtained. The new fractional splines have all properties of the polynomial splines, with the exception of compact support when the order $\alpha$ is noninteger. The main advantage of this construction is that we can build the wavelet bases parameterized by the continuously varying regularity parameter $\alpha$.

*Fractional B-spline*.—It was shown in the literature (1–3) that this family interpolates between the integer degrees of polynomial B-splines, and that they allow a fractional order of approximation. The fractional B-spline is defined as follows:

$$\beta_+^{\alpha}(x) = \frac{\Delta_+^{\alpha+1} x_+^{\alpha}}{\Gamma(\alpha+1)} = \frac{\sum_{k=0} (-1)^k \binom{\alpha+1}{k} (x-k)_+^{\alpha}}{\Gamma(\alpha+1)} \quad (1)$$

where Euler's gamma function has the form:

$$\Gamma(\alpha+1) = \int_0^{+\infty} x_e^{\alpha} - x_{dx} \quad (2)$$

and

$$(x-k)_+^{\alpha} = \max(x-k,0)^{\alpha} \quad (3)$$

The forward fractional finite difference operator of order $\alpha$ is defined by:

$$\Delta_+^{\alpha} f(x) = \sum_{k=0}^{+\infty} (-1)^k \binom{\alpha}{k} f(x-k) \quad (4)$$

where

$$\binom{\alpha}{k} = -\frac{\Gamma(\alpha+1)}{\Gamma(k+1)\Gamma)\Gamma - k+1)} \quad (5)$$

The above-defined B-splines fulfill the convolution property:

$$\beta_+^{\alpha 1*} \beta_+^{\alpha 2} = \beta_+^{\alpha 1+\alpha 2} \quad (6)$$

In addition, the centered fractional B-splines of degree $\alpha$ are given by:

$$\beta_*^{\alpha}(x) = \frac{1}{\Gamma(\alpha+1)} \sum_{k \in Z} (-1)^k \left| \begin{matrix} \alpha+1 \\ k \end{matrix} \right| \left| x-k \right|_*^{\alpha} \quad (7)$$

where $|x|_*^{\alpha}$ has the following form:

$$|x|_*^{\alpha} = \begin{cases} \dfrac{|x|\alpha}{-2\sin\left(\dfrac{\pi}{2}\alpha\right)}, \ \alpha \text{ not even} \\ \dfrac{x^{2n} \log x}{(-1)^{1+n}\pi}, \ \alpha \text{ even} \end{cases} \quad (8)$$

*Fractional B-spline wavelets*.—The definition of the fractional B-spline wavelets is presented below:

$$\psi_+^{\alpha}\left(\frac{x}{2}\right) = \sum_{k \in Z} \frac{(-1)^k}{2^{\alpha}} \sum_{l \in Z} \binom{\alpha+1}{l} \beta_*^{2\alpha+1}(1+k-l)\beta_+^{\alpha}(x-k) \quad (9)$$

The fractional splines wavelets obey:

$$\int_{-\infty}^{+\infty} x^n \psi_+^{\alpha}(x)dx = 0 \quad (10)$$

and the Fourier transform fulfills the following relations:

$$\hat{\psi}_+^{\alpha}(\varpi) = C(j\varpi)^{\alpha+1}, \text{ as } \varpi \longrightarrow 0 \quad (11)$$

and

$$\hat{\psi}_*^{\alpha}(\varpi) = C(j\varpi)^{\alpha+1}, \text{ as } \varpi \longrightarrow 0 \quad (12)$$

Downloaded from https://academic.oup.com/jaoac/article/89/6/1538/5657781 by ANKARA UNIVERSITESI user on 11 December 2021

Here, $\hat{\psi}_*^{\alpha}(\varpi)$ is symmetric. The last formulas show us that the fractional spline wavelets look like a fractional derivative operator.

### *CWT-Zero-Crossing Approach*

If a binary mixture of 2 analytes, *X* and *Y*, is considered and if the absorbance value of this binary mixture is measured at $\lambda_i$, then the following equation emerges:

$$\mathrm{Am}_{\lambda i} = \alpha\lambda_i\ C_X + \beta\lambda_i\ C_Y \qquad (13)$$

Here, $\mathrm{Am}_{\lambda i}$ represents the absorbance of the binary mixture at wavelength $\lambda_i$, and the coefficients $\alpha\lambda_i$ and $\beta\lambda_i$ are absorptivities of the *X* and *Y* analytes. $C_X$ and $C_Y$ denote the concentrations of the analytes. After CWT is applied on Equation 13, we obtain:

$$\mathrm{CWT}(\mathrm{Am}_{\lambda i}) = \mathrm{CWT}(\alpha\lambda_i\ C_X) + \mathrm{CWT}(\beta_{\lambda i}\ C_Y) \quad (14)$$

If CWT $(\alpha_{\lambda i}\ C_X) = 0$, then we obtain the following result:

$$\mathrm{CWT}(\mathrm{Am}_{\lambda i}) = \mathrm{CWT}(\beta_{\lambda i}\ C_Y) \qquad (15)$$

Equation 15 shows that CWT amplitudes of compound *Y* in a binary mixture are dependent only on the concentration of $C_Y$ and are independent of the concentration of compound *X* in the binary mixture. The calibration graphs can be obtained by plotting $\mathrm{CWT}(\mathrm{Am}_{\lambda i})$ signals versus the concentration of $C_Y$. The above procedure is repeated for *X* analyte in the binary mixture. In our paper, the Mexican hat wavelet function given by the following formula:

$$\psi(x) = \left(\frac{2\pi^{-1/4}}{\sqrt{3}}\right)\left(1-x^2\right)e^{-x^2/2} \qquad (16)$$

is considered. As can be seen, this function is proportional to the second derivative function of the Gaussian probability density function.

### *Linear Regression Analysis*

A linear regression equation between 2 variables, concentration and absorbance, for the spectrophotometric determination of the *X* analyte at $\lambda_i$ wavelength can be defined as:

$$A_{Xi} = b_{Xi}C_X + a_{Xi} \qquad (17)$$

where $A_{Xi}$ is the absorbance of the *X* analyte at $\lambda_i$ wavelength, $C_X$ is the concentration of the *X* analyte (the concentration units are μg/mL in this study), $b_{Xi}$ is the slope of the linear regression equation, and $a_{Xi}$ is the intercept of the regression model.

*Multivariate spectral calibration*.—If the absorbance values of a mixture of 2 analytes (*X* and *Y*) are measured at *n* wavelengths ($\lambda_i = 1, 2, \ldots\ldots, n$), the following set of equations can be written for a 2-component analysis. In the matrix terms, the multiequation component can be formulated as:

$$\begin{bmatrix} A_{mix_1} \\ A_{mix_2} \\ \ldots\ldots \\ \ldots\ldots \\ A_{mix_n} \end{bmatrix} = \begin{bmatrix} b_{X_1}\ b_{Y_1} \\ b_{X_2}\ b_{y_2} \\ \ldots\ldots \\ \ldots\ldots \\ b_{X_n}\ b_{y_n} \end{bmatrix} * \begin{bmatrix} C_X \\ C_Y \end{bmatrix} + \begin{bmatrix} a_{XY_1} \\ a_{XY_2} \\ \ldots\ldots \\ \ldots\ldots \\ a_{XY_n} \end{bmatrix} \qquad (18)$$

where $A_{mix_1}$, $A_{mix_2}$, ……, $A_{mix_n}$ are the absorbances of the mixture of *X* and *Y* analytes at selected wavelengths (from $\lambda_1$ to $\lambda_n$); $b_{x_1}$, $b_{x_2}$, …$b_{x_n}$, and $b_{y_1}$, $b_{y_2}$, …$b_{y_n}$ are the slopes of *n* linear regression equations of *X* and *Y*, corresponding to selected wavelengths, respectively; and $a_{XY_1}, a_{XY_2}, \ldots$, and $a_{XY_n}$ are the sums of intercepts of linear regression equations at *n* wavelengths $\left(a_{XY_1} = a_{X_1} + a_{Y_1}, a_{XY_2} = a_{X2} + a_{Y2} \ldots \text{and } a_{XY_n} = a_{X_n} + a_{Y_n}\right)$.

The above equation system can be simplified as:

$$\begin{bmatrix} A_{mix_1} - a_{XY_1} \\ A_{mix_2} - a_{XY_2} \\ \ldots\ldots\ \ldots\ldots \\ \ldots\ldots\ \ldots\ldots \\ A_{mix_n} - a_{XY_n} \end{bmatrix} = \begin{bmatrix} b_{X_1}\ b_{Y_1} \\ b_{X_2}\ b_{Y_2} \\ \ldots\ldots\ \ldots\ldots \\ \ldots\ldots\ \ldots\ldots \\ b_{X_n}\ b_{Y_n} \end{bmatrix} * \begin{bmatrix} C_X \\ C_Y \end{bmatrix} \qquad (19)$$

or in a compact form, it becomes:

$$(A_{mix} - a_{XYZ})_{n\times 1} = K_{n\times 2} * C_{2\times 1} \qquad (20)$$

As explained in the above calibration method, the matrix of the slope values is called the matrix K:

$$K_{n\times 2} = \begin{bmatrix} b_{X_1}\ b_{Y_1} \\ b_{X_2}\ b_{Y_2} \\ \ldots\ldots\ \ldots\ldots \\ \ldots\ldots\ \ldots\ldots \\ b_{X_n}\ b_{Y_n} \end{bmatrix} \qquad (21)$$

The matrixes, $(A_{mix} - a)_{n\times 1}$ and $K_{n\times 2}$, are multiplied by the inverse $(K^{-1})_{2\times n}$ of the matrix $K_{n\times 2}$ and can be written as:

$$(K^{-1})_{2\times n}\,(A_{mix} - a)_{n\times 1} = (K^{-1})_{2\times n}\,K_{n\times 2} * C_{2\times 1} \qquad (22)$$

The concentration of the *X* and *Y* compounds in a binary mixture can be calculated by using the following formula:

$$C_{2\times 1} = [(K^{-1})_{2\times n}\,K_{n\times 2}]^{-1} * [(K^{-1})_{2\times n}\,(A_{mix} - a_{XY})_{n\times 1}] \quad (23)$$

In this case, the MLRC model involves the use of linear algebra, also known as matrix mathematics. This calibration model can be applied to the quantitative analysis of 2-component mixtures or multicomponent mixtures.

## Experimental

During the study, the light exposure was minimized throughout all operations because of the light sensitivity of

Downloaded from https://academic.oup.com/jaoac/article/89/6/1538/5657781 by ANKARA UNIVERSITESI user on 11 December 2021

LAC. The photodegradation procedure was entirely carried out in a room lighted with 60 W red lamp.

### *Instruments*

Absorption spectra were recorded in the wavelength range of 190–450 nm in a 10 mm quartz cell by using a Perkin-Elmer (Milano, Italy) Lambda 40P spectrophotometer with the following settings: scan rate, 1 nm/s; time response, 1 s; spectral bandwidth, 1 nm. For the spectral acquisition and elaboration, the ultraviolet (UV) Winlab 2.70.01 software (Perkin-Elmer) was used. The photodegradation study was performed in an irradiation cabinet (Suntest CPS+; Heraeus, Italy), which fulfills ICH recommendations for light source characteristics. The irradiation system was equipped with a xenon arc lamp showing an emission spectrum very similar to solar light. Close control of the temperature was obtained by a cooling device to keep the degradation rate independent of temperature. The temperature was maintained at 21°C.

### *Calculations*

The mathematical calculations and the wavelet transform procedure were carried out by using Microsoft Excel and the wavelet toolbox in MATLAB 7.0 (MathWorks, Inc., Natick, MA).

### *Reagents*

Pure LAC was kindly contributed by GlaxoSmithKline S.p.A. (Verona, Italy). The photodegradation product was isolated by direct oxidation of LAC by irradiating a 200 mg/mL hexane suspension of the drug with the xenon lamp until the absorbance peak at 300 nm, due to LAC only, disappeared. After an irradiation time of 60 h, the solid was filtered and washed with pure hexane. The purity and identity of LACD was confirmed by gas chromatography/mass spectrometry analysis, exhibiting a molecular peak at *m/z* 455 and characteristic fragments at *m/z* 382, 326, and 252, in agreement with a literature report (6). Ethanol (95%) was of spectrophotometric grade (J.T. Baker, Deventer, The Netherlands). Lacipil 4 and 6 mg (GlaxoSmithKline S.p.A.) pharmaceutical specialties were obtained commercially.

### *Standard Solutions*

Standard sets of LAC and LACD in the concentration range of 5.0–40.0 and 0.5–10.0 μg/mL, respectively, were prepared in ethanol. These standards were used to obtain the calibration between transformed signals and concentrations. A calibration set containing 20 standard binary mixtures with LAC and LACD distributed in 5 concentration levels was prepared to build the PLS regression model. A prediction set containing 25 standard binary mixtures in 5 concentration levels was used to validate the defined methods. Mexican hat function and MLRC were applied to the above-mentioned mixture samples after FWT.

### *Photodegradation Tests*

Photodegradation procedures were carried out in the Suntest cabinet by constant irradiation in the wavelength range 270–800 nm. Radiant power was set at 350 W/m$^2$, corresponding to an energy value of 21 kJ/min/m$^2$. This value was chosen because degradation follows linear kinetics when exposure is limited to low-enough values of radiant power, as suggested by preceding studies (6). The inner temperature was fixed at 25°C.

The photostability of the LAC pharmaceutical form was tested by exposing 5 tablets to artificial light and analyzing them at different time intervals. For this purpose, the tablets were weighed and reduced to a fine powder. An amount exactly corresponding to the average tablet weight was suspended in ethanol, and the volume was made up to 20 mL. The suspension was sonicated for 10 min, and then filtered with a polytetrafluoroethylene (PTFE) 0.45 μm membrane filter. One mL of the filtrate was diluted to 10 mL with ethanol and analyzed.

## Results and Discussion

The absorption spectra of LAC and its degradation product are presented in Figure 1A. These spectra show that the simultaneous determination of LAC and LACD by ordinary or derivative spectrophotometry, using measurements at discrete wavelengths, could not be satisfactorily performed because of the extensive overlap of the peaks. The spectral interference was very critical for LACD, because of the relatively higher concentration of LAC. To bypass this difficulty, the FWT approach was applied to the absorption spectra of LAC and LACD in the spectral range of 225–430 nm. The next step was to apply the Mexican hat function and MLRC to the coefficients obtained by FWT. These hybrid approaches gave successful results for the quantitative evaluation of LAC and LACD in samples.

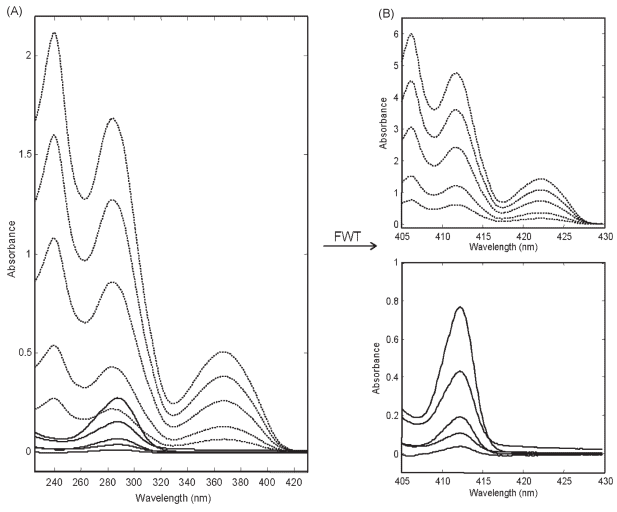



**Figure 1. Original absorption spectra (A) and their corresponding FWT spectra (B) of 5.08, 10.16, 20.32, 30.48, and 40.64 μg/mL LAC (……) and 0.51, 1.02, 2.04, 4.08, and 8.16 μg/mL LACD (—).**

Downloaded from https://academic.oup.com/jaoac/article/89/6/1538/5657781 by ANKARA UNIVERSITESI user on 11 December 2021

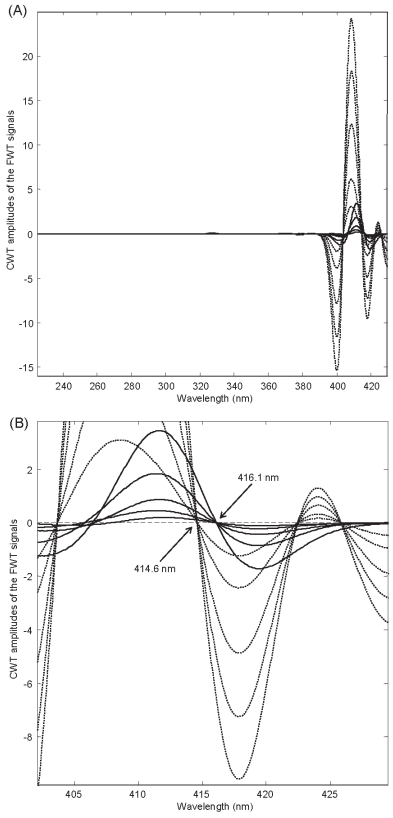



**Figure 2. The CWT spectrum (A) and its detailed form (B) of the FWT signals of 5.08, 10.16, 20.32, 30.48, and 40.64 μg/mL LAC (……) and 0.51, 1.02, 2.04, 4.08, and 8.16 μg/mL LACD (—).**

### *FWT Approach*

The absorption spectra of the drug and its degradation product were transferred to MATLAB as signal vectors consisting of 2048 elements. The vectors were processed with a special program of fractional wavelets. A series of parameters were tested, and we retained those giving the highest amplitude, small range, and a denoising condition. In our case, the values of the optimal parameters were found to be J = 3 (the depth of the decomposition), the fractional parameter $\alpha = 2.5$, the type +O. FWT coefficients were plotted versus the original wavelength points as shown in Figure 1B.

### *CWT Approach*

To determine LAC and LACD in their mixture samples, FWT data vectors were processed by the Mexican hat function at the scaling factor $a = 40$. CWT spectra were obtained by plotting the CWT $C_{a,b}$ coefficients versus wavelengths, as seen in Figure 2A and B.

By using the zero-crossing technique, CWT calibration functions were obtained by measuring the CWT amplitudes at 416.1 nm for LAC and 414.6 nm for LACD, and their statistical results were summarized in Table 1. In spite of the low quantity of LACD, a good linearity for both compounds was observed in the working concentration range. These calibration functions were used for the quantitative evaluation of LAC and LACD.

### *MLRC Approach*

As a comparison method, MLRC applied to the FWT coefficients was used. For this reason, the 15-wavelength set at the critical points, which correspond to the maximum, shoulder, and minimum in the spectral range 411.0–412.4 nm, was selected for the construction of the individual linear regression for pure LAC and LACD. As indicated in Table 2, 15 linear regression equations for LAC and LACD in the concentration range of 5.08–40.64 and 0.51–8.16 μg/mL, respectively, were obtained by measuring the FWT amplitude values at the wavelength set. The equation set was obtained as follows:

$$\lambda_1 = 411.0 \text{ nm}, \text{Amix1} = 0.1123\ C_{LAC} + 0.0796\ C_{LACD} + 0.0360$$
$$\lambda_2 = 411.1 \text{ nm}, \text{Amix2} = 0.1136\ C_{LAC} + 0.0815\ C_{LACD} + 0.0353$$
$$\lambda_3 = 411.2 \text{ nm}, \text{Amix3} = 0.1146\ C_{LAC} + 0.0836\ C_{LACD} + 0.0377$$
$$\lambda_4 = 411.3 \text{ nm}, \text{Amix4} = 0.1154\ C_{LAC} + 0.0856\ C_{LACD} + 0.0386$$
$$\lambda_5 = 411.4 \text{ nm}, \text{Amix5} = 0.1161\ C_{LAC} + 0.0875\ C_{LACD} + 0.0363$$
$$\lambda_6 = 411.5 \text{ nm}, \text{Amix6} = 0.1167\ C_{LAC} + 0.0893\ C_{LACD} + 0.0345$$
$$\lambda_7 = 411.6 \text{ nm}, \text{Amix7} = 0.1167\ C_{LAC} + 0.0908\ C_{LACD} + 0.0370$$
$$\lambda_8 = 411.7 \text{ nm}, \text{Amix8} = 0.1169\ C_{LAC} + 0.0922\ C_{LACD} + 0.0338$$

**Table 1. Linear regression analysis and corresponding results**

| Wavelength, nm | Linear regression function | r[a] | SE(r)[b] | SE(n)[c] | SE(m)[d] | LOD[e], μg/mL | LOQ[f], μg/mL |
|---|---|---|---|---|---|---|---|
| 416.1 | $S^g = 0.1627\ C_{LAC} + 0.0303$ | 1.0000 | 0.0180 | 0.0154 | 0.0006 | 0.2868 | 0.9559 |
| 414.6 | $S = 0.1951\ C_{LACD} - 0.0002$ | 1.0000 | 0.0027 | 0.0018 | 0.0004 | 0.0355 | 0.1182 |

[a] r = Correlation coefficient of linear regression function.
[b] SE(r) = Standard error of correlation coefficient.
[c] SE(n) = Standard error of intercept.
[d] SE(m) = Standard error of slope.
[e] LOD = Limit of detection.
[f] LOQ = Limit of quantitation.
[g] S = CWT amplitude of the FWT spectra.

Downloaded from https://academic.oup.com/jaoac/article/89/6/1538/5657781 by ANKARA UNIVERSITESI user on 11 December 2021

**Table 2. Regression statistics and their results**

| Wavelength, nm | Linear regression equation[a] | r[b] | SE(m)[c] | SE(n)[d] | SE(r)[e] | Linear regression equation[a] | r | SE(m) | SE(n) | SE(r) |
|---|---|---|---|---|---|---|---|---|---|---|
| 411.0 | $A = 0.1123\ C_{LAC} + 0.0315$ | 0.9999 | 0.0181 | 0.0007 | 0.0210 | $A = 0.0796\ C_{LACD} + 0.0045$ | 0.9955 | 0.0185 | 0.0044 | 0.0273 |
| 411.1 | $A = 0.1136\ C_{LAC} + 0.0305$ | 0.9999 | 0.0170 | 0.0007 | 0.0198 | $A = 0.0815\ C_{LACD} + 0.0047$ | 0.9958 | 0.0183 | 0.0043 | 0.0270 |
| 411.2 | $A = 0.1146\ C_{LAC} + 0.0324$ | 0.9999 | 0.0179 | 0.0007 | 0.0209 | $A = 0.0836\ C_{LACD} + 0.0053$ | 0.9960 | 0.0181 | 0.0043 | 0.0268 |
| 411.3 | $A = 0.1154\ C_{LAC} + 0.0331$ | 0.9999 | 0.0189 | 0.0008 | 0.0220 | $A = 0.0856\ C_{LACD} + 0.0055$ | 0.9962 | 0.0183 | 0.0043 | 0.0270 |
| 411.4 | $A = 0.1161\ C_{LAC} + 0.0314$ | 0.9999 | 0.0179 | 0.0007 | 0.0209 | $A = 0.0875\ C_{LACD} + 0.0049$ | 0.9963 | 0.0183 | 0.0043 | 0.0270 |
| 411.5 | $A = 0.1167\ C_{LAC} + 0.0303$ | 1.0000 | 0.0167 | 0.0007 | 0.0195 | $A = 0.0893\ C_{LACD} + 0.0042$ | 0.9966 | 0.0181 | 0.0043 | 0.0267 |
| 411.6 | $A = 0.1167\ C_{LAC} + 0.0324$ | 0.9999 | 0.0184 | 0.0007 | 0.0214 | $A = 0.0908\ C_{LACD} + 0.0046$ | 0.9966 | 0.0181 | 0.0043 | 0.0268 |
| 411.7 | $A = 0.1169\ C_{LAC} + 0.0293$ | 1.0000 | 0.0159 | 0.0006 | 0.0185 | $A = 0.0922\ C_{LACD} + 0.0045$ | 0.9969 | 0.0177 | 0.0042 | 0.0262 |
| 411.8 | $A = 0.1167\ C_{LAC} + 0.0289$ | 1.0000 | 0.0156 | 0.0006 | 0.0182 | $A = 0.0934\ C_{LACD} + 0.0045$ | 0.9970 | 0.0176 | 0.0042 | 0.0260 |
| 411.9 | $A = 0.1163\ C_{LAC} + 0.0306$ | 0.9999 | 0.0170 | 0.0007 | 0.0198 | $A = 0.0943\ C_{LACD} + 0.0041$ | 0.9970 | 0.0177 | 0.0042 | 0.0261 |
| 412.0 | $A = 0.1157\ C_{LAC} + 0.0312$ | 0.9999 | 0.0174 | 0.0007 | 0.0202 | $A = 0.0950\ C_{LACD} + 0.0037$ | 0.9971 | 0.0176 | 0.0042 | 0.0260 |
| 412.1 | $A = 0.1151\ C_{LAC} + 0.0306$ | 0.9999 | 0.0171 | 0.0007 | 0.0199 | $A = 0.0955\ C_{LACD} + 0.0041$ | 0.9972 | 0.0174 | 0.0041 | 0.0257 |
| 412.2 | $A = 0.1141\ C_{LAC} + 0.0329$ | 0.9999 | 0.0186 | 0.0007 | 0.0217 | $A = 0.0955\ C_{LACD} + 0.0046$ | 0.9972 | 0.0174 | 0.0041 | 0.0257 |
| 412.3 | $A = 0.1132\ C_{LAC} + 0.0324$ | 0.9999 | 0.0185 | 0.0007 | 0.0216 | $A = 0.0954\ C_{LACD} + 0.0044$ | 0.9972 | 0.0174 | 0.0041 | 0.0257 |
| 412.4 | $A = 0.1120\ C_{LAC} + 0.0311$ | 0.9999 | 0.0176 | 0.0007 | 0.0205 | $A = 0.0950\ C_{LACD} + 0.0041$ | 0.9973 | 0.0171 | 0.0041 | 0.0253 |

[a] A = FWT amplitude.
[b] r = Correlation coefficient of the linear regression function.
[c] SE(m) = Standard error of slope.
[d] SE(n) = Standard error of intercept.
[e] SE(r) = Standard error of the correlation coefficient.



Downloaded from https://academic.oup.com/jaoac/article/89/6/1538/5657781 by ANKARA UNIVERSITESI user on 11 December 2021

**Table 3. Concentration set for the PLS calibration**

| | Concn, mg/mL | |
|---|---|---|
| No. | LAC | LACD |
| 1 | 5.08 | 0.00 |
| 2 | 5.08 | 0.51 |
| 3 | 10.16 | 0.00 |
| 4 | 40.64 | 0.51 |
| 5 | 20.32 | 0.00 |
| 6 | 20.32 | 1.02 |
| 7 | 30.48 | 0.00 |
| 8 | 10.16 | 2.04 |
| 9 | 40.64 | 0.00 |
| 10 | 30.48 | 2.04 |
| 11 | 0.00 | 0.51 |
| 12 | 20.32 | 4.08 |
| 13 | 0.00 | 1.02 |
| 14 | 10.16 | 8.16 |
| 15 | 0.00 | 2.04 |
| 16 | 30.48 | 8.16 |
| 17 | 0.00 | 4.08 |
| 18 | 40.64 | 8.16 |
| 19 | 0.00 | 8.16 |
| 20 | 20.32 | 0.51 |

**Table 4. Predicted concentration values of the mixture samples**

| Predicted concn, μg/mL | | | |
|---|---|---|---|
| FWT + MLRC | | FWT + CWT | |
| LAC | LACD | LAC | LACD |
| 4.77 | 0.54 | 5.30 | 0.54 |
| 9.97 | 0.50 | 10.49 | 0.53 |
| 20.40 | 0.49 | 20.79 | 0.55 |
| 30.38 | 0.55 | 30.95 | 0.51 |
| 40.32 | 0.53 | 40.90 | 0.48 |
| 4.96 | 1.08 | 5.35 | 1.04 |
| 10.17 | 0.99 | 10.55 | 1.03 |
| 20.60 | 0.98 | 20.85 | 1.06 |
| 30.58 | 1.06 | 31.01 | 0.99 |
| 40.52 | 1.02 | 40.96 | 0.95 |
| 4.81 | 2.15 | 5.44 | 2.09 |
| 10.01 | 2.07 | 10.54 | 2.09 |
| 20.45 | 2.06 | 20.84 | 2.11 |
| 30.42 | 2.15 | 31.00 | 2.05 |
| 40.37 | 2.10 | 40.95 | 1.96 |
| 5.40 | 3.95 | 5.51 | 4.13 |
| 10.61 | 3.87 | 10.60 | 4.12 |
| 21.04 | 3.86 | 20.90 | 4.15 |
| 31.02 | 3.94 | 31.06 | 4.08 |
| 40.96 | 3.89 | 41.01 | 3.99 |
| 4.75 | 8.27 | 5.42 | 8.19 |
| 9.95 | 8.18 | 10.52 | 8.18 |
| 20.38 | 8.18 | 20.82 | 8.21 |
| 30.36 | 8.26 | 30.98 | 8.14 |
| 40.30 | 8.22 | 40.93 | 8.06 |

$$\lambda_9 = 411.8 \text{ nm}, \text{Amix9} = 0.1167\ C_{LAC} + 0.0934\ C_{LACD} + 0.0334$$
$$\lambda_{10} = 411.9 \text{ nm}, \text{Amix10} = 0.1163\ C_{LAC} + 0.0943\ C_{LACD} + 0.0347$$
$$\lambda_{11} = 412.0 \text{ nm}, \text{Amix11} = 0.1157\ C_{LAC} + 0.0950\ C_{LACD} + 0.0348$$
$$\lambda_{12} = 412.1 \text{ nm}, \text{Amix12} = 0.1151\ C_{LAC} + 0.0955\ C_{LACD} + 0.0347$$
$$\lambda_{13} = 412.2 \text{ nm}, \text{Amix13} = 0.1141\ C_{LAC} + 0.0955\ C_{LACD} + 0.0374$$
$$\lambda_{14} = 412.3 \text{ nm}, \text{Amix14} = 0.1132\ C_{LAC} + 0.0954\ C_{LACD} + 0.0368$$
$$\lambda_{15} = 412.4 \text{ nm}, \text{Amix15} = 0.1120\ C_{LAC} + 0.0950\ C_{LACD} + 0.0351$$

The MLRC algorithm was applied to the above equation set to construct the calibration. This MLRC approach was used for the quantitative analysis of the binary mixtures containing LAC and LACD, as was explained in the section above on *Multivariate spectral calibration*. It was observed that this method is a powerful tool with very simple mathematical content for quantitative analysis of binary and multiple mixtures.

A standard PLS calibration was applied as an independent method on the original absorption spectra of LAC and LACD in their mixtures. PLS is recognized to be a powerful method in the analysis of multicomponent complex mixtures, even when applied to complex mixtures characterized by a severe overlapping. PLS allows individual analysis of each component by correlating the variation in the component information with respect to the spectral data. For this purpose, the concentration and absorption data from a calibration set consisting of 20 mixtures (Table 3) were used to build the PLS calibration. Mean recoveries and relative standard deviations (RSD) from the assay of the calibration mixtures (Table 4) were 99.5 and 1.52% for LAC and 102.9 and 8.44% for LACD, respectively. RSD for LACD is an unacceptable value for a satisfactory quantitative evaluation of the photoproduct in real samples. This poor precision was probably caused by the very low content of LACD compared to the parent drug, providing undetectable or uncorrelated analytical signals.

### *Quantitative Analysis and Validation*

The Mexican hat function and MLRC based on FWT coefficients were validated by analyzing synthetic mixtures of LAC and LACD, and the obtained results are given in Table 4. In spite of the low concentration of LACD, we were able to process the data by using the Mexican hat function and MLRC

Downloaded from https://academic.oup.com/jaoac/article/89/6/1538/5657781 by ANKARA UNIVERSITESI user on 11 December 2021

**Table 5. Accuracy and precision data obtained by the proposed approaches**

| Mixture, μg/mL | | Recovery, % | | | |
|---|---|---|---|---|---|
| | | FWT+ MLRC | | FWT + CWT | |
| LAC | LACD | LAC | LACD | LAC | LACD |
| 5.08 | 0.51 | 93.8 | 106.3 | 104.3 | 105.1 |
| 10.16 | 0.51 | 98.1 | 98.0 | 103.3 | 104.2 |
| 20.32 | 0.51 | 100.4 | 95.2 | 102.3 | 106.9 |
| 30.48 | 0.51 | 99.7 | 107.6 | 101.5 | 100.2 |
| 40.64 | 0.51 | 99.2 | 103.0 | 100.6 | 94.7 |
| 5.08 | 1.02 | 97.7 | 105.7 | 105.4 | 101.6 |
| 10.16 | 1.02 | 100.1 | 97.0 | 103.8 | 101.1 |
| 20.32 | 1.02 | 101.4 | 95.8 | 102.6 | 103.5 |
| 30.48 | 1.02 | 100.3 | 104.4 | 101.7 | 97.1 |
| 40.64 | 1.02 | 99.7 | 100.1 | 100.8 | 93.4 |
| 5.08 | 2.04 | 94.7 | 105.6 | 107.2 | 102.6 |
| 10.16 | 2.04 | 98.5 | 101.6 | 103.7 | 102.3 |
| 20.32 | 2.04 | 100.6 | 100.7 | 102.5 | 103.6 |
| 30.48 | 2.04 | 99.8 | 105.3 | 101.7 | 100.3 |
| 40.64 | 2.04 | 99.3 | 102.8 | 100.8 | 96.1 |
| 5.08 | 4.08 | 106.4 | 96.8 | 108.4 | 101.1 |
| 10.16 | 4.08 | 104.4 | 94.8 | 104.3 | 101.0 |
| 20.32 | 4.08 | 103.5 | 94.5 | 102.9 | 101.6 |
| 30.48 | 4.08 | 101.8 | 96.6 | 101.9 | 100.0 |
| 40.64 | 4.08 | 100.8 | 95.4 | 100.9 | 97.9 |
| 5.08 | 8.16 | 93.4 | 101.3 | 106.8 | 100.4 |
| 10.16 | 8.16 | 97.9 | 100.3 | 103.5 | 100.3 |
| 20.32 | 8.16 | 100.3 | 100.2 | 102.5 | 100.6 |
| 30.48 | 8.16 | 99.6 | 101.3 | 101.6 | 99.8 |
| 40.64 | 8.16 | 99.2 | 100.7 | 100.7 | 98.7 |
| Mean | | 99.6 | 100.4 | 103.0 | 100.6 |
| SD[a] | | 2.91 | 3.99 | 2.10 | 3.11 |
| RSD[b] | | 2.92 | 3.97 | 2.04 | 3.09 |

[a] SD = Standard deviation.
[b] RSD = Relative standard deviation.

based on the CWT approach. No significant difference between the results of the methods was found.

The predicted concentrations by the above 2 methods are much closer to each other as well as to the actual concentrations shown in Table 5. Accuracy and precision were evaluated by analysis of triplicate samples. Recovery means and RSDs were 99.6–103.0 and 2.04–3.97%, respectively, for both products. These results clearly indicated that the 2 proposed methods are suitable for quantitative evaluations of the investigated compounds.

LAC commercial formulations were subjected to analysis by the proposed procedures. When applied to pharmaceutics, the methods required only a simple and rapid sample preparation, which avoided any detectable photodegradation during the entire manipulation process. The recorded results were in agreement with the content of drug declared on confection labels. The photodegradation product content of assayed pharmaceutical specialties was found to be lower than 1.1%.

## Conclusions

In this study, 2 new approaches were developed for the simultaneous analysis of the binary mixture systems of LAC and its photodegradation product, LACD. Although the individual spectra of LAC and LACD overlap in the 225–430 nm range and LACD is present in very low content,

Downloaded from https://academic.oup.com/jaoac/article/89/6/1538/5657781 by ANKARA UNIVERSITESI user on 11 December 2021

the Mexican hat function, CWT, and MLCR approaches using the FWT coefficients give successful quantitative analysis of the mentioned mixtures. In addition, the 2 methods described in this paper do not require a chemical pretreatment, such as a prior separation step. Results also showed that the developed methods are more reliable than classical spectrophotometric methods. Finally, all of the developed methods can be readily applied to the quantitative analysis of the binary mixtures of interest.

## References


(1) Zanocco, A.L., Diaz, L., Lopez, M., Nunez-Vergara, L.J., & Squella, J.A. (1992) *J. Pharm. Sci.* **81**, 920–924

(2) Ragno, G., Veronico, M., & Vetuschi, C. (1995) *Int. J. Pharm.* **119**, 115–119

(3) Sridhar, K., Sastry, C.S.P., Reddy, M.N., Sankar, D.G., & Rama Srinivas, K. (1997) *Anal. Lett.* **30**, 121–126

(4) Ragno, G., & Vetuschi, C. (1998) *Die Pharmazie* **53**, 628–631

(5) Ragno, G., Garofalo, A., & Vetuschi, C. (2002) *J. Pharm. Biomed. Anal*. **27**, 19–24

(6) De Filippis, P., Bovina, E., Da Ros, L., Fiori, J., & Cavrini, V. (2002) *J. Pharm. Biomed. Anal.* **27**, 803–812

(7) Rossato, P., Scandola, M., Pughnagh, F., & Grossi, P. (1992) *Org. Mass Spectrom*. **27**, 1261–1265

(8) Rossato, P., Scandola, M., & Grossi, P. (1993) *J. Chromatogr.* **647**, 155–156

(9) Meyanathan, S.N., Rama Sarma, G.V.S., & Suresh, B. (1999) *Indian Drugs* **36**, 9–15

(10) ICH Harmonized Tripartite Guideline, Photostability Testing of New Drug Substance and Products (1996) *Federal Register* **62**, 27115–27122

(11) Unser, M., & Blu, T. (1998) *Proc. SPIE Wavelets Applications in Signal and Image Processing VII*, Denver, CO, Vol. 3813, pp 422–431

(12) Unser, M., & Blu, T. (2000) *SIAM Review* **42**, 43–67

(13) Unser, M., & Blu, T. (2000) *Proceedings of the Twenty-Fifth IEEE International Conference on Acoustics, Speech, and Signal Processing (ICASSP'00)*, IEEE, Istanbul, Turkey, June 5–9, Vol. I, pp 512–515

(14) Dinç, E., & Baleanu, D. (2006) *Spectrochim. Acta, Part A* **63**, 631–638

(15) Van De Ville, D., Blu, T., & Unser, M. (2005) *IEEE Transactions on Image Processing* **14**, 1798–1813

(16) Walczak, B. (2000) *Wavelets in Chemistry*, F.T. Chan & A.K.M. Leung (Eds), Elsevier Press, Amsterdam, The Netherlands, p. 241

(17) Daubechies, I. (1992) *Ten Lectures on Wavelets*, Society for Industrial and Applied Mathematics, Philadelphia, PA

(18) Leung, A.K., Chau, F.T., & Gao, J. (1998) *J. Chemom. Intell. Lab. Sys.* **43**, 165–184

(19) Lu, X.O., Liu, H.D., Kang, J.W., & Cheng, J. (2003) *Anal. Chim. Acta* **484**, 201–210

(20) Dinç, E., & Baleanu, D. (2003) *Talanta* **59**, 707–717

(21) Dinç, E., & Baleanu, D. (2004) *J. AOAC Int.* **87**, 360–365

(22) Dinç, E., & Baleanu, D. (2004) *J. AOAC Int.* **87**, 834–841

(23) Dinç, E., Ozdemir, A., & Baleanu, D. (2005) *Talanta* **65**, 36–47

(24) Dinç, E., Baleanu, D., & Üstündağ, O. (2003) *Spectrosc. Lett.* **36**, 341–355

(25) Dinç, E., Ozdemir, A., & Baleanu, D. (2005) *J. Pharm. Biomed. Anal.* **37**, 569–575

(26) Dinç, E. (2003) *J. Pharm. Biomed. Anal.* **33**, 605–615

(27) Dinç, E., & Ozdemir, A. (2004) *Die Pharmazie* **59**, 700–705

(28) Dinç, E., & Ozdemir, A. (2005) *Chem. Pharm. Bull*. **53**, 899–906

(29) Üstündağ, U., & Dinç, E. (2003) *Die Pharmazie* **58**, 623–628

(30) Dinç, E., & Baleanu, D. (2005) *Rev. Chim.* **56**, 937–942


Downloaded from https://academic.oup.com/jaoac/article/89/6/1538/5657781 by ANKARA UNIVERSITESI user on 11 December 2021